A preliminary study of chemical property and thermal stability of potassium chloride encapsulated in starch-alginate matrix

A preliminary study of chemical property and thermal stability of potassium chloride encapsulated in starch-alginate matrix

Ying Si Chen, Siew Wei Phang*, Anis Suhaila Shuib

School of Engineering, Taylor's University, Subang Jaya, Malaysia

*Corresponding author: Siewwei.Phang@taylors.edu.my, eunicepsw@gmail.com

Abstract: A potassium controlled-release fertilizer was fabricated in a starch-alginate matrix by using calcium chloride as a cross-linker. 16 formulas were designed with varying amounts of alginate and potassium chloride with the same amount of starch and calcium chloride, and most of the formulas can form beads successfully. High sodium alginate and low potassium chloride assembled better shape and higher encapsulation efficiency. The highest encapsulation efficiency ratio of starch, sodium alginate, and potassium chloride was 5:1:10 in the 16 formulas. The bonding of alginate and starch, and calcium chloride were evidenced by FTIR, and the study of TGA revealed good thermal stability and compatibility between the polymers and potassium chloride.

Keywords: potassium fertilizer, Controlled-release, Hydrogel, Starch-Alginate

1.Introduction

The world population is estimated to increase by one third or 2.3 billion and reach 9.5 billion by 2050 and food demand also increases as the population blooming [1], [2]. Many countries are using fertilizer heavily to increase the food production, but the improper use of fertilizer which had led to environmental pollution, such as soil salinity, heavy metal accumulation, water eutrophication and accumulation of nitrate, and even greenhouse effect due to the air gases containing nitrogen and sulphur [3], [4].

Controlled-release fertilizer (CRF) is a fertilizer specially designed to mitigate nutrient loss and run-off [5], reduce the pollution of soil, water and atmospheric relieve toxicity and stress to plants [6], also solve the issue of fertilizer combustion [5]. Active nutrients of CRF are released to plants for fertilization in a controlled, delayed manner with sequential synchronization of the required nutrients [6], which improved the property and safety of chemicals. As a result, they supply higher nutrient use efficiency and higher yields compared to conventional fertilizers [6]. There were some latest research on CRFs, such as polyurethane coatings which are modified castor oil and starch [7], poly (lactic acid-glycolic acid) and soy separation protein [8], biopolymer coatings which are liquefied corncob bio-based polyurethane, starch-based polyurethane (SPU) coating [7], wheat starch, polyethylene alcohol (PVA) and puffed soils, yak dung hydro-char (HC) [9], sawdust and tea waste biochar [10] and also a polysulfide-matrix [11], vitreous [12], iron-based metal-organic frameworks [13], municipal bio-wastes [14], hydrogel like tamarind kernel gum [14], chitosan (CS) and polyethylene alcohol (PVA) [15] and so on.

Potassium is one of the essential nutrients among nitrogen, phosphorus and potassium (NPK) fertilizers, Different from nitrogen and phosphorus, potassium is not part of the chemical structure of plants, so it does not exist in the form of organic compounds instead of an anionic state which mainly in the plant branches, leaves and other tissue organs [16]. It is essential for many plant-growth processes, such as enzyme activation, stomatal activity, photosynthesis, transport of sugar, water and nutrient, synthesis of protein and starch, improve crop quality, etc. [17]. The effects of inadequate potassium supply can cause reduced yield potential and quality, causing losses, especially during critical developmental stages of short periods of deficiency, which rob the profits of the farmers [17]. Hence, it is significant to controlled-release the potassium nutrients to promote the high quality and high yield of crops and improves fertilization benefits.

Hydrogels are widely used in the controlled release of compounds due to the facility with which they disperse in the matrix, alginate and alginate-starch hydrogels have been studied widely for compound encapsulation [18], [19]. Alginate reacts with polyvalent metal cations, such as calcium ions in aqueous media to generate strong gels and insoluble polymers [20]. Sodium alginate (SA) forms calcium alginate hydrogels through Ca^{2+} crosslinking, and calcium chloride ($CaCl_2$) is the commonly used ion cross-linker. Ca^{2+} replace Na^{+} in the sodium alginate G segment producing the structure called "egg-box" to convert the sodium alginate water solution into a gel [21]. Starch is a biodegradable, non-toxic, inexpensive, and abundantly available material [18]. Before crosslinking in $CaCl_2$ solution, adding starch to SA can improve the stability of beads [22]. The starch-rich alginate beads are more resistant to deformation than the starch-free ones without changing their mechanical properties [23].

The encapsulation of urea, phosphate fertilizer was synthesized with starch and SA, $CaCl_2$ as a cross-linked with SA [24], [25]. Hence, the project is a preliminary study on bio-degradable polymer matrix using varying potassium chloride. The hydrogels were successfully prepared, and the chemical property and thermal stability were investigated.

2.Materials and Methods

2.1Materials

Analytical grade C.P. Sodium-Alginate (SA), Granular C.P. calcium chloride dihydrate ($CaCl_2 \cdot 2H_2O$) and A.R. potassium chloride (KCl) were obtained from R&M Chemical, UK. Meanwhile cassava starch (food grade), brand Cap Kapal ABC, manufactured in Thailand, purchased off the shelf from supermarket in Malaysia.

2.2 Preparation of hydrogel beads

The preparation method was discussed in detailed by the author in the previous paper [24], [26], as well as the formulations designed. Total of 16 formulations was prepared, as shown in **Table 1**.

Starch, SA and KCl were mixed in 100 ml of distilled water. The solution was stirred continuously for 30 minutes at a speed of 600 RPM by using the Thermos Scientific Magnetic Stirrer (Thermos Scientific MSH-300) at 40°C. Calcium chloride was dissolved in 100 ml of distilled water as a crosslink solution. The starch-SA-KCl mixture solution was dripped into the $CaCl_2$ solution. The formed starch-potassium-alginate (St -K-Alg) beads were rinsed with distilled water and filtered with 200 mesh screens. The beads were dried for 24 hours in an oven (Memmert UN75) at 70°C.

Table 1 Formulations of starch-alginate hydrogel beads

#	Starch (% ,w/v)	SA (% ,w/v)	KCl (%, w/v)	$CaCl_2$(M)	Encapsulation efficiency

S1	10	0.5	5	0.75	68.06%
S2	10	1.0	5	0.75	93.53%
S3	10	1.5	5	0.75	89.64%
S4	10	2.0	5	0.75	99.47%
S5	10	0.5	10	0.75	47.48%
S6	10	1.0	10	0.75	52.63%
S7	10	1.5	10	0.75	63.01%
S8	10	2.0	10	0.75	70.91%
S9	10	0.5	15	0.75	29.23%
S10	10	1.0	15	0.75	31.85%
S11	10	1.5	15	0.75	42.71%
S12	10	2.0	15	0.75	52.41%
S13	10	0.5	20	0.75	29.77%
S14	10	1.0	20	0.75	41.06%
S15	10	1.5	20	0.75	44.76%
S16	10	2.0	20	0.75	51.88%

2.3 Sample Characterization

2.3.1 Encapsulation efficiency. The encapsulation efficiency of the St-Alg-K beads is calculated as the equation (1) [26]

$$\text{yield}(\%) = \frac{W_B}{W_R} \times 100\% \quad (1)$$

The amount of raw material which were starch, sodium alginate and potassium chloride will be weighted by using electronic balance and recorded as W_R, the beads were also weighted after drying at a constant weight and recorded as W_B.

2.3.2 Transform Infrared (FTIR) Spectroscopy. The chemical interaction of the beads was found using a FTIR (Spectrum 100, Perkin Elmer). The chemical bonds were found when the wavelength range was set from 4000 cm^{-1} to 650 cm^{-1} by using ATR (Attenuated Total Reflectance) sampling method [25]. A total of 18 scans were done including the pure starch, sodium alginate.

2.3.3 Thermogravimetry Analysis (TGA). TGA (TGA 8000, Perkin Elmer) was operating from 30 °C to 800 °C to determine the thermal degradation at a fixed rate of 20 °C /min in the nitrogen atmosphere [24]. 5 to 10 mg pure starch, sodium alginate were tested respectively with the samples. Three replications of all the samples were selected randomly for the analysis.

3.Results and discussion

3.1 Physical shape

The shape of the Ca–alginate beads produced using the extrusion-dripping method was mainly influenced by the liquid properties (i.e., surface tension and viscosity of the alginate and gelling solutions) and the process conditions (i.e., collecting distance). During the fabrication, the shape of the beads was affected by the dropping speed, collecting distance via observation.

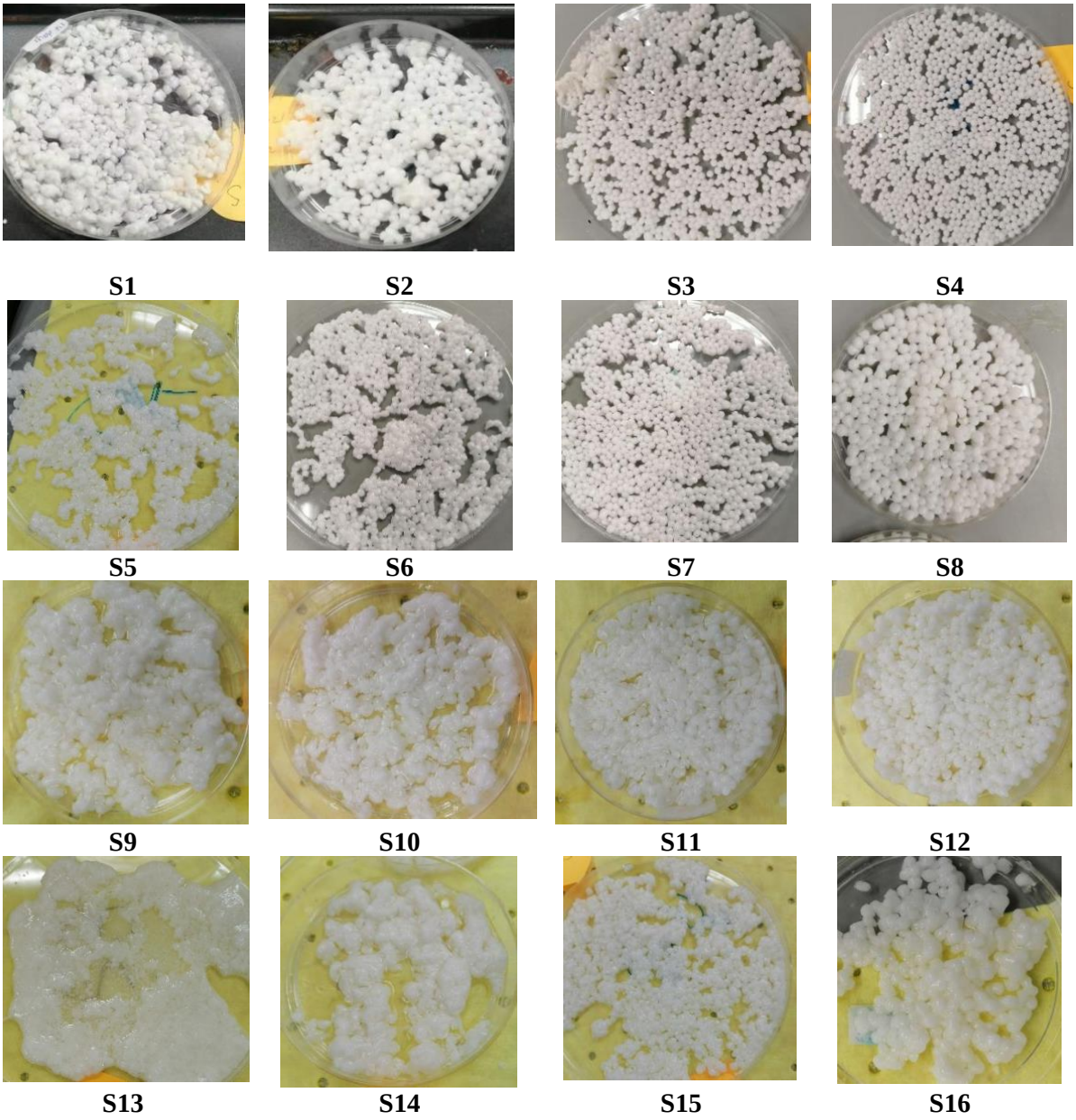

Figure 1 16 samples before dry

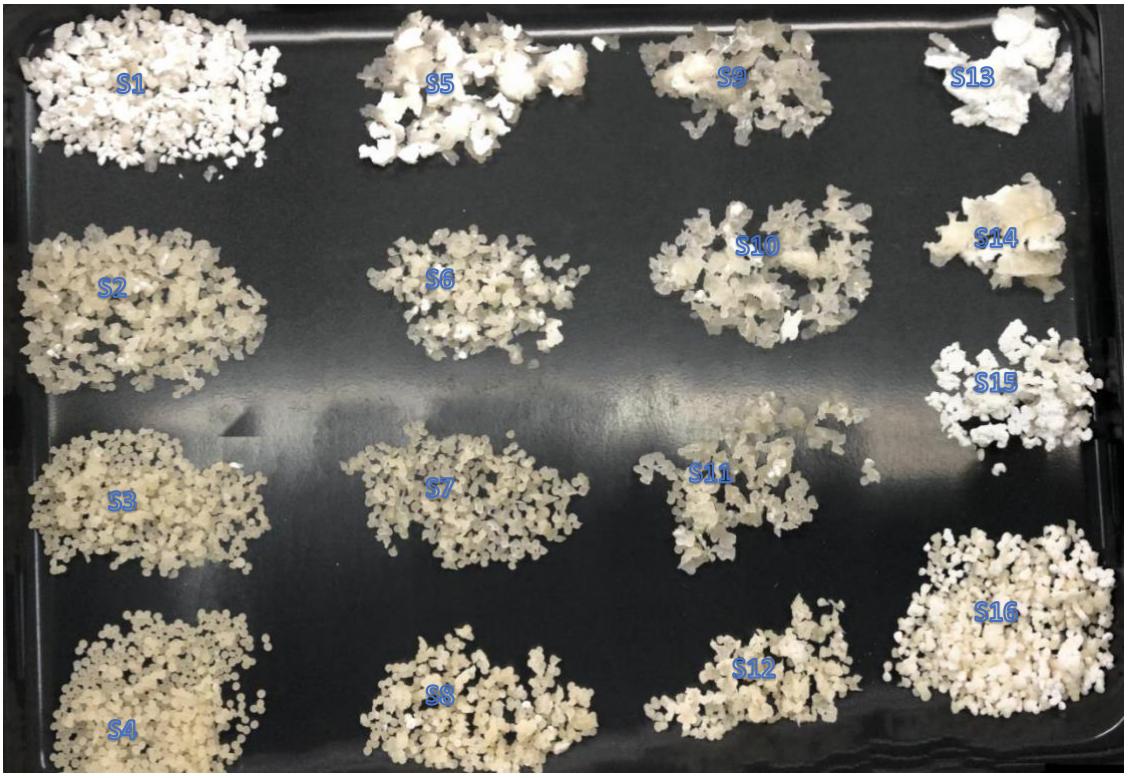

Figure 2 16 samples after dry

Starch is a filler material to encapsulate compounds that bind to the carboxyl groups of alginate, creating a uniform matrix, and improving adhering capacity and bead formation[18] as well as responsible for spherical hydrogel beads [25]. Corresponding to the formulas in Table 1, the same ratio of starch and calcium chloride in each sample, so SA and potassium chloride content were the main factors affecting the matric affect the shape of the beads in this study.

Four groups which are S1-S4, S5-S8, S9-S12, and S13-S16 were divided from 16 samples based on the different levels of potassium chloride, 5% w/v, 10% w/v, 15% w/v, 20% w/v respectively. In the 5% w/v-level KCl group, S4 has a spherical shape, more even, tighter, and more elastic compared to S1 with the increase in the radio of alginate. The same results were demonstrated among the 10% w/v, 15% w/v, and 20% w/v level groups due to the effect of alginate content. According to the different levels of sodium alginate, 4 groups 0.5% w/v (S1, S5, S9, S13), 1% w/v (S2, S6, S10, S14), 1.5% w/v (S3, S7, S11, S15), 2% w/v (S4, S8, S12, S16) were divided from 16 samples respectively. S16 showed less even, tight, elastic beads than S12, S8, and S4 with the increase of the potassium chloride when the SA content is at the 2% w/v alginate level. S4 and S8 had a tighter shape than S12 and S16 due to the lower potassium chloride content, while S16 and S12 were garlic shapes compared to round shapes S4 and S8. Among the 0.5% w/v SA level group, the shapeless sample with the increasing of potassium chloride while S13 can't form a bead shape and S5, S9 and S13 were fragile. Similar to 0.5% w/v SA and 2% w/v SA level, higher potassium chloride with a more fragile, shapeless appearance of the beads.

As mentioned above, starch played a filler role which was responsible for shaping a spherical hydrogel bead around 15 wt% [25]. At the same level of starch, some of the samples (S3, S4, S7, S8) can keep a spherical shape, most of them were garlic shapes. There might be low SA content samples with a lower viscosity which is mentioned by previous research that SA is responsible for increasing viscosity to form a teardrop shape during sample synthesis [25]. According to the observation, Starch-Alginate-KCl solution with low viscosity samples will be easier to drop into the calcium chloride solution by using the dropper, and the end of beads will be stretched because of the gravity therefore a garlic shape forms. Once the Starch-Alginate- KCl beads are dropped into the calcium chloride solution, they will shrink inward obviously with the low-level SA samples. Conversely, the high-level SA samples can keep a similar size after cross-linking with the calcium chloride. Larger droplets extruded from the

dropper to form larger beads due to an increase in the mixture viscosity, while the loss of wall material was relatively small in $CaCl_2$ solution during the formation of beads[27].

Therefore, the bead's size might be decided by the cross-linking effect with SA under the same level of calcium chloride. Moreover, the high-level SA samples were easier to separate while the low-level SA is the trend to stick together before and after drying, which verifies lower-level SA with less cross-linking on the surface of the bead, but more starch on the surface.

Overall, better shape, more elastic, and less fridge of the beads with higher alginate and lower potassium chloride when the starch and calcium chloride content are at the same level.

3.2 Encapsulation efficiency

As shown in Table 1, the encapsulation efficiency decreased with the increased level of potassium chloride, from 5% w/v, 10% w/v, 15% w/v to 20% w/v and at the same level of potassium chloride, the encapsulation efficiency increased with the increasing SA. In line with the research data from [28,29], a higher encapsulation efficiency can be achieved with the increment of the SA content [26].

The previous research found that 1 g of SA required 0.128 g of $CaCl_2$ determined by using a potentiometric titration method [30]. Therefore, 0.75M $CaCl_2$ crosslinking with 2% w/v SA can be considered as sufficient.

Starch added to SA solution before gelling in $CaCl_2$ solution can improve the stability of microspheres [22]. Consistent starch interacted with alginate only through hydrogen bonding[26]. As shown in S4, 10% w/v starch mixed with 2% w/v SA is 99.47% encapsulation efficiency which is almost 100% mean 10% w/v starch to 2% w/v SA can make a good encapsulation. The percentage yield of starch–alginate–Ca^{2+} beads has not been affected by the increases in starch contents but by the alginate amount and cross-linker concentration[26].

In the previous study, the author described the “molecular pockets” that are formatted by starch and SA bonded with each other via physical forces between their network of macromolecular chains and then the varying size mesh occupied by the active ingredient[31]. So the higher SA and bond with starch means more physical force between them and creative more “molecular pockets” which can be occupied by more active ingredient. When the active ingredient increased, there was not enough mesh for them which might be the reason for the increase in potassium chloride, the encapsulation efficiency decreased. Singh et al. (2009b) research found that the constant feed of active ingredients there did not affect the entrapment efficiency which oppositely proved our finding [32].

3.3 Transform Infrared (FTIR) Spectroscopy

The S4 was selected randomly to compare with the pure SA and starch to study the interactions between polymers. Figure 3 demonstrates the spectra of SA, starch, S4. The characteristic absorption bands of SA, starch and S4 were 3291cm^{-1}, 3270 cm^{-1} and 3383 cm^{-1}, respectively due to the presence of O-H stretching vibrations [33], [26].

The wavenumber of 2934 cm^{-1}, 2933 cm^{-1}, 2976 cm^{-1} of SA, starch, S4 respectively attributed to the C–H asymmetric stretching vibration ring [25], [26], [33], [34]. For starch, the band around 1644 cm^{-1} was attributed to the O–H bending vibration of water molecules adsorbed in the amorphous region of starch granules. The band of around 1077 cm^{-1} to 1150 cm^{-1} is pertain to the asymmetric stretching vibration of C–O in C–O–H structure [26], [33].

For SA, and the asymmetric (1594 cm^{-1}) and symmetric (1408 cm^{-1}) stretching of the carboxylate group –COO was observed in the region of 1620 - 1654 cm^{-1} and 1414 - 1464 cm^{-1} respectively which align with the previous studies [26], [33].

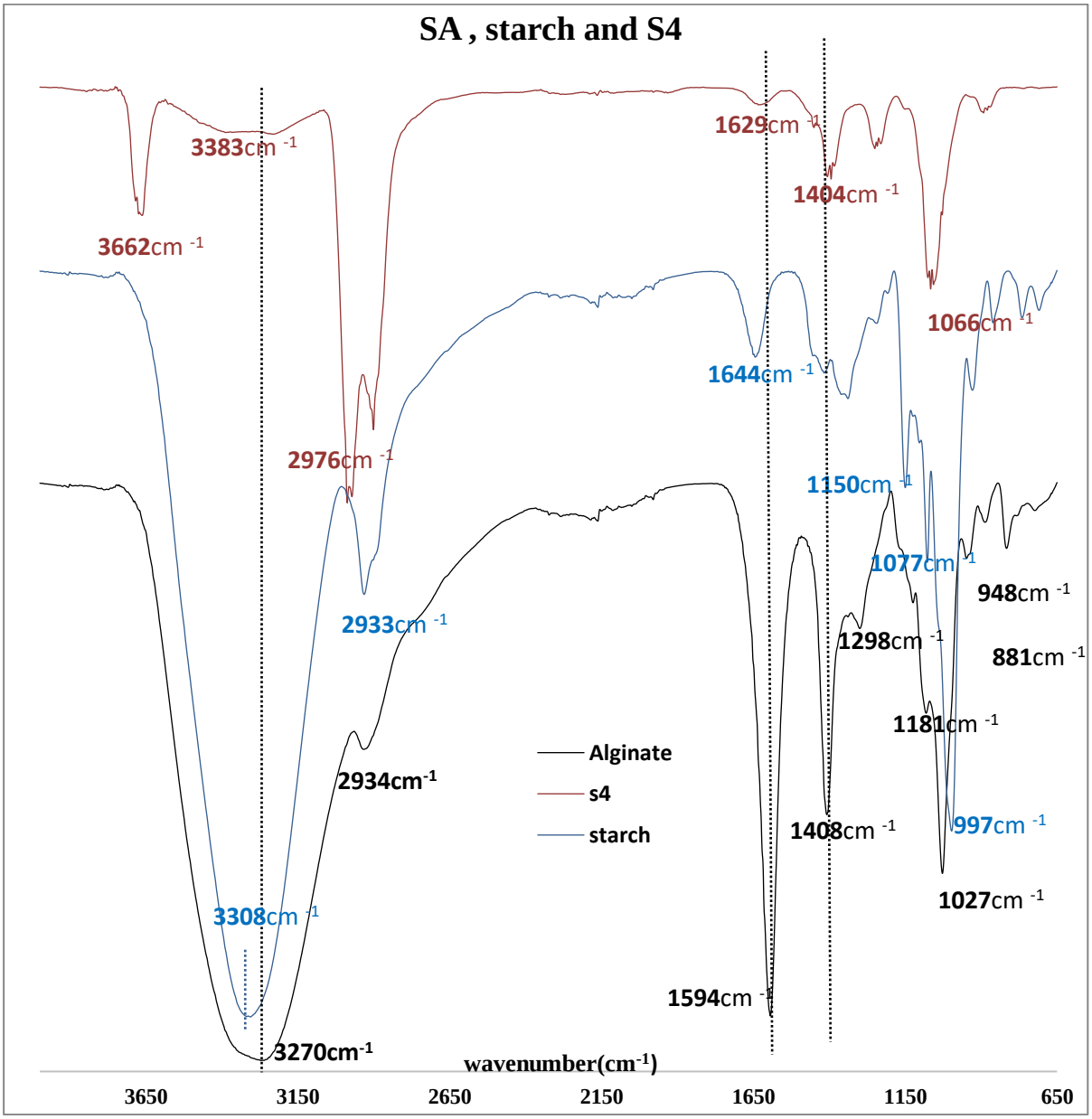

Figure 3 FTIR spectra of SA, starch, S4 and S13

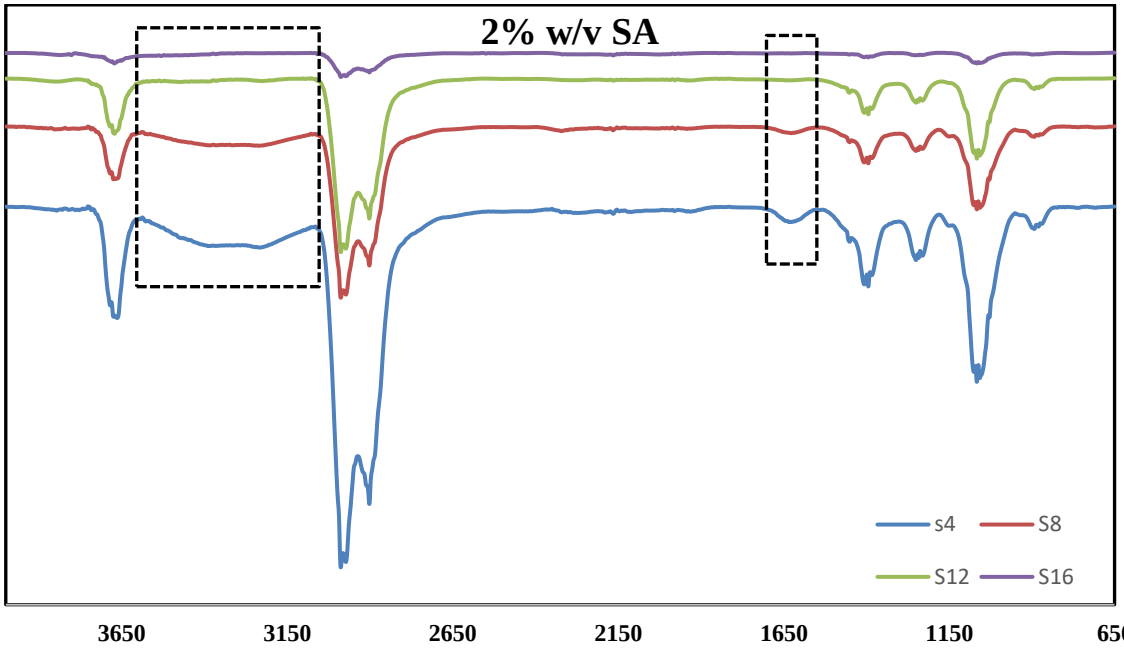

Figure 4 Wavenumber of function groups at 2% w/v SA level

From 2900 cm^{-1} to 3600 cm^{-1} led to the overlapped peak positions based on the hydroxyl groups which was due to the similar chemical structures of the SA [35]. The –OH stretching vibration peak of calcium alginate had a higher wavenumber (3306 cm^{-1} to 3342 cm^{-1}) than SA (3270 cm^{-1}). This was probably due to a negative effect on bond formation involving adjacent hydroxyl groups because of conformational changes of alginate after reacting with Ca^{2+} [36]. The result also aligned with the finding from [37] that –OH and COO– groups from SA molecular chain can interact with –OH groups of starch which wavenumber increase with increasing of starch [38]. The hydroxyl peak shifted proving the interaction of starch and alginate also reported by the [25].

The presence of obvious peak of COO– symmetric stretching (1408cm^{-1}) and asymmetric stretching **(**1594 cm^{-1}**)** stretching absorption from SA and weaker symmetric stretching band in 1404 cm^{-1} of S4 is supporting the presence carboxylate anion of SA and calcium alginate [32]. The decreased wavenumber the of COO– (from 1408 cm^{-1} to 1404 cm^{-1}) and reduction intensity of the peaks were mainly caused by the combination of starch with alginate which H-bonds may have been formed between them [25] and the cross-linking of SA by Ca^{2+} [36]. As shown in Figure 3, a new peak in 3660 cm^{-1} showed in S4, which attribute to H-bond[39], with the decrease of the –OH bending from starch, possible due to strong H-bond between starch and SA. By comparing FTIR spectra of S4 and SA, it can be confirmed that crosslinking between alginate and calcium was successful and a weak COO– asymmetric stretching was found in 1629 cm^{-1} [40]. The wave number 1629 cm^{-1} might be attributed to bounded water presented in starch and to COO– asymmetric stretching of SA [35].

It was reported that with the increase of KCl, the intensity of hydroxyl peak decreased due to the strong interaction between PVA and SA as well as KCl via intra/inter molecular hydrogen bonding with adjacent OH groups [41]. Also, the peak corresponding C=O stretching was slightly shift towards higher wavenumber with decrease in intensity, supports the interaction of KCl with PVA/NaAlg blend [41]. The intensity of hydroxyl and C=O peaks decreased with the increased of KCl (Figure 4), assuming the same ratio of starch, SA will be same transmittance, the changing intensity can prove the potassium chloride were successfully encapsulated in the matrix.

3.4 TGA

Thermo-gravimetric analyzer (TGA) used to analyze the changes in weight as function of time and temperature which usually characterize moisture, volatile contents, and thermal stability of the

compounds [25], [42]. Normally, when a biomaterial is heated to higher temperature it decomposes into CO_2, CO, NOx and H_2O [43].

S1, S4, S13, and S16 were compared according to the various starch and SA ratio in the 16 formulation which represented the highest starch ratio, highest SA ratio, and lowest SA ratio, lowest starch ratio respectively.

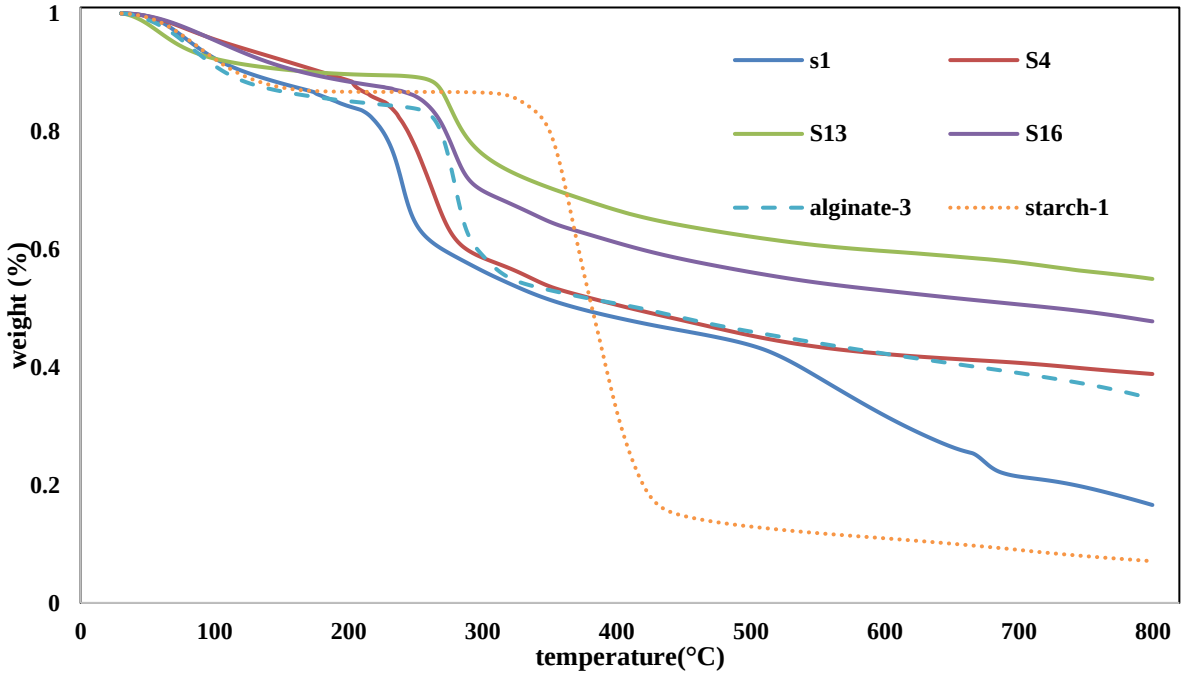

Figure 5 TGA graph of S1,S4,S13,S16 , starch and SA

In general, similar thermal degradation profile of the samples as shown in Figure 5 under 600 °C. There was a 0% weight loss range of starch (170°C to 300°C) and SA (200°C to 250°C), which in parallel with the horizontal axis. The curve of SA was used for comparison where its shape is similar to all the samples' curves except for S1, maybe due to both SA and starch being hydrophilic and heterocyclic polymers containing –OH groups thus showed similar thermal degradation [38], [44]. As shown in Figure 6, 16 samples were classified into 4 different SA levels, the curves' trend is similar to the increase in SA amount. Not only S1 but also S5 are different from the other samples which both belonged to the low SA and low potassium chloride group. With the addition of potassium chloride, the thermal stability of starch-alginate bead was improved as shown the difference between S1 and S13, S4 and S16 are similar to the research by [34].

According to [37], the TGA thermal behaviour of SA/Starch blends was undergo two-stage thermal degradation. Figure 5 showed that the mass loss percentage of S1 and S13 was higher than S4 and S16 below 200°C, similar to SA and starch which are assigned to dehydration of loosely bound water and low molecular weight compound [45] or the interaction between different forms of water molecules and polysaccharides [46]. The mass degradation of samples was between 180 and 320°C and can be attributed to the structural decomposition of starch and SA in the polymer matrix, as hydrophilic and heterocyclic polymers, which showed the similar thermal degradation because of the –OH groups [44]. The temperature at the second stage weight loss percentage is higher, which might be due to the high content of starch where the methylene groups of starch underwent degradation only in the second stage [38]. Or might be the addition of potassium chloride improved the thermal stability which was found in Figure 5 that the increase of the potassium chloride corresponded to the decrease of weight loss percentage from 250°C.

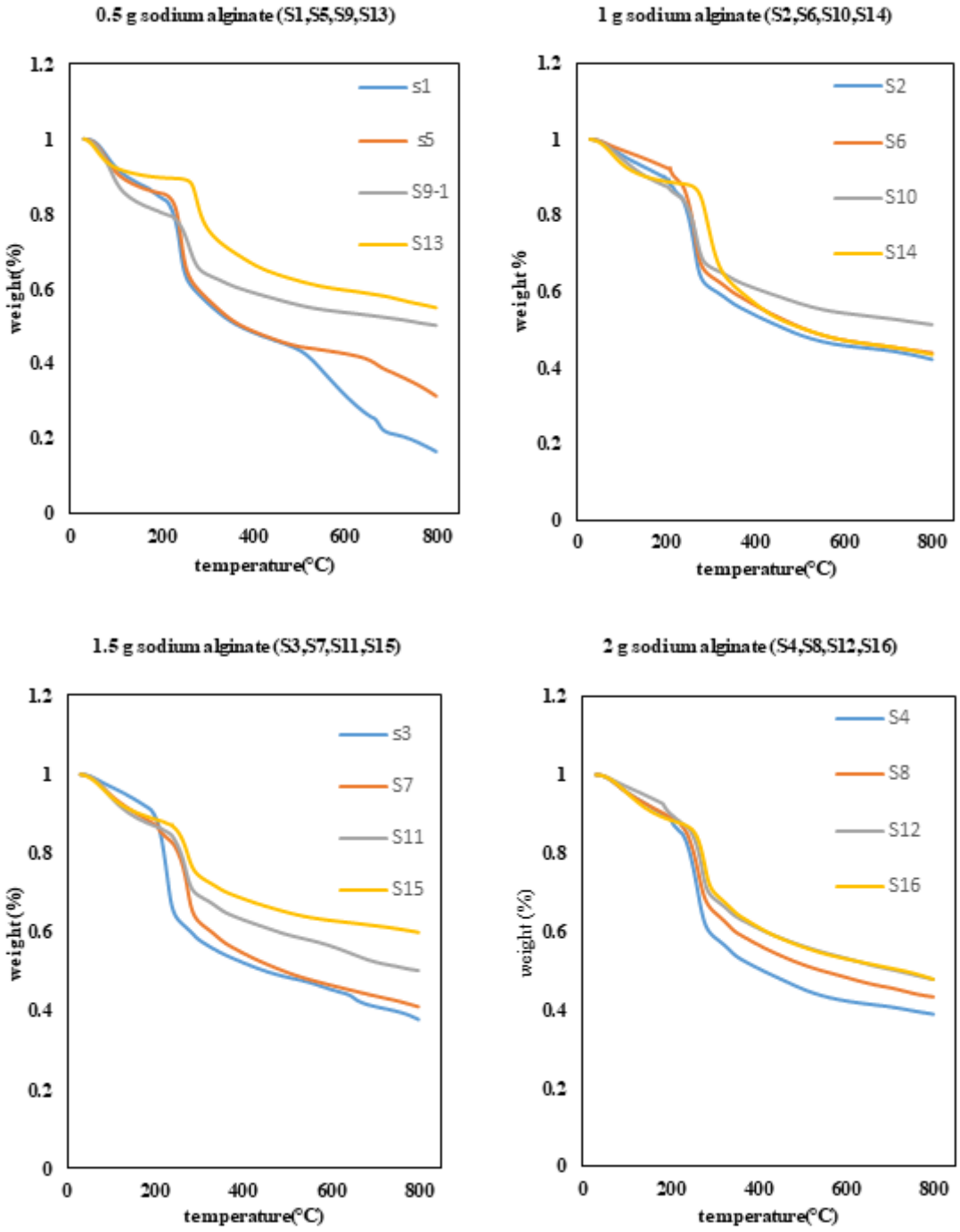

Figure 6 TGA graph of 16 samples

4.Conclusion

Overall, potassium chloride was encapsulated in starch-alginate matrix successfully, higher SA and lower KCl can form a better shape of bead and higher encapsulation efficiency. When the ratio of starch,

SA and KCl was 10:2:5, almost 100% encapsulation efficiency, but there were no beads formed when the ratio of SA to KCl was 1:40, 1:30, 1:20 with the constant starch. The chemical property has been investigated by FTIR and confirmed the crosslinking between SA and $CaCl_2$ and the bonding between SA and starch. The thermal stability has also been investigated by TGA and the addition of potassium chloride improved the thermal stability. In the future, the release behavior and biodegradability will be further investigated and optimize the ratio of KCl and SA to achieve a maximum %K.

References

[1] Bapat S, Koranne V, Shakelly N, Huang A, Sealy M P, Sutherland J W, Rajurkar K P, and Malshe A P 2022 Cellular agriculture: an outlook on smart and resilient food agriculture manufacturing *Smart and Sustainable Manufacturing Systems* **6** 1-11

[2] Lawrencia D, Wong S K, Low D Y S, Goh B H, Goh J K, Ruktanonchai U R, Soottitantawat A, Lee L H and Tang S Y 2021 Controlled release fertilizers: a review on coating materials and mechanism of release *Plants* **10** 1–26

[3] Savci S 2012 An agricultural pollutant: chemical fertilizer *International Journal of Environmental Science and Development* **3** 73–80

[4] Kalia A, Sharma S P, Kaur H and Kaur H 2020 *Novel nanocomposite-based controlled-release fertilizer and pesticide formulations: Prospects and challenges* (Elsevier Inc.) 99

[5] Rajan M, Shahena S, Chandran V and Mathew L 2021 Controlled release of fertilizers - concept, reality, and mechanism *Controlled Release Fertilizers for Sustainable Agriculture* 41–56

[6] Shaviv A and Mikkelsen R L 1993 Controlled-release fertilizers to increase efficiency of nutrient use and minimize environmental degradation - a review *Fertilizer Research* **35** 1–12

[7] Liao Y, Liu L, Wang M, Li L X, Cao B, Wang H and Huang W Q 2021 Preparation and properties of starch-based polyurethane/montmorillonite composite coatings for controlled-release fertilizer *Polym Compos* **42** 2293–304

[8] Yu Z, Yang Y, Wang C, Shi G, Xie J, Gao B, Li Y C, Wan Y, Cheng D, Shen T, Hou S, Zhang S, Ma X, Yao Y, Tang Y and Chen J 2021 Nano-soy-protein microcapsule-enabled self-healing biopolyurethane-coated controlled-release fertilizer: preparation, performance, and mechanism *Mater Today Chem* **20** 100413

[9] Wu W, Yan B, Sun Y, Zhong L, Lu W and Chen G 2021 Potential of yak dung-derived hydrochar as fertilizer: mechanism and model of controlled release of nitrogen *Science of the Total Environment* **781** 146665

[10] Jayarathna, M.K.N.W.and W M U K R 2021 Biochar based slow-release urea fertilizer : production and assessing the effects on growth of lowland rice and nitrogen dynamics in an alfisol *Tropical Agricultural Research* **32** 168–78

[11] Ribeiro C, do Valle S F, Giroto A S, Reis H P G and Guimarães G G F 2021 Synergy of phosphate-controlled release and sulfur oxidation in novel polysulfide composites for sustainable fertilization *J Agric Food Chem* **69** 2392-402

[12] Labbilta T, Ait-el-mokhtar M, Abouliatim Y, Khouloud M, Meddich A and Mesnaoui M 2021 Elaboration and characterization of vitreous fertilizers and study of their impact on the rowth, photosynthesis and yield of wheat (Triticum durum l.) *Materials* **14** 1–19

[13] Du Y, Xu X, Ma F and Du C 2021 Solvent-free synthesis of iron-based metal-organic frameworks (MOFs) as slow-release fertilizers *Polymers (Basel)* **13** 1–10

[14] Evon P, Labonne L, Padoan E, Vaca-Garcia C, Montoneri E, Boero V and Negre M 2021 A new composite biomaterial made from sunflower proteins, urea, and soluble polymers obtained from industrial and municipal biowastes to perform as slow release fertiliser *Coatings* **11** 1–22

[15] Vo P T, Nguyen H T, Trinh H T, Nguyen V M, Le A T, Tran H Q and Nguyen T T T 2021 The nitrogen slow-release fertilizer based on urea incorporating chitosan and poly(vinyl alcohol) blend *Environ Technol Innov* **22** 101528

[16] Tiwari S P, Joshi O P, Vyas A K and Billore S D 2002 Potassium nutrition in yield and quality improvement of soybean *Potassium for sustainable crop production* 307–20

[17] Prajapati K 2012 The importance of potassium in plant growth – a review *researchgate.net* **1** 177–86
[18] Feltre G, Sartori T, Silva K F C, Dacanal G C, Menegalli F C and Hubinger M D 2020 Encapsulation of wheat germ oil in alginate-gelatinized corn starch beads: Physicochemical properties and tocopherols' stability *J Food Sci* **85** 2124–33
[19] Feltre G, Almeida F S, Sato A C K, Dacanal G C and Hubinger M D 2020 Alginate and corn starch mixed gels: Effect of gelatinization and amylose content on the properties and in vitro digestibility *Food Research International* **132** 109069
[20] Fazilah A, Maizura M, Abd Karim A, Bhupinder K, Rajeev B, Uthumporn U and Chew S H 2011 Physical and mechanical properties of sago starch - alginate films incorporated with calcium chloride *Int Food Res J* **18** 1027–33
[21] Chan L W, Jin Y and Heng P W S 2002 Cross-linking mechanisms of calcium and zinc in production of alginate microspheres *Int J Pharm* **242** 255–8
[22] Oyeagu U, Nwuche C, Ogbonna C and Ogbonna J 2018 Addition of fillers to sodium alginate solution improves stability and immobilization capacity of the resulting calcium alginate beads *Iran J Biotechnol* **16** 67–73
[23] Zafeiri I, Beri A, Linter B and Norton I 2020 Mechanical properties of starch-filled alginate gel particles *Carbohydr Polym* **255** 117373
[24] Phang S W, Sin L T, Bee S, Tee T and How Y Y 2018 Release behavior and degradation study of controlled-released urea encapsulated in starch- alginate hydrogel *Advanced Technology in Engineering & Management - ICATEM 19 (CONFERENCE)* 1–6
[25] Phang S W, Sin L T, Bee S T, Low J Y and Tee T T 2018 Release behaviour study on controlled-release phosphorous fertilizer encapsulated by starch-alginate superabsorbent composite *Journal of Engineering Science and Technology* **13** 82–94
[26] Singh B, Sharma D K and Gupta A 2009 The controlled and sustained release of a fungicide from starch and alginate beads *J Environ Sci Health B* **44** 113–22
[27] Wu Z, Guo L, Qin S and Li C 2012 Encapsulation of R. planticola Rs-2 from alginate-starch-bentonite and its controlled release and swelling behavior under simulated soil conditions *J Ind Microbiol Biotechnol* **39** 317–27
[28] Phang S W, Sin L T, Bee S-T, Low J Y and Tee T-T 2018 Release behaviour study on controlled-release phosphorous fertilizer encapsulated by starch-alginate superabsorbent composite *Journal of Engineering Science and Technology* 82–94
[29] Singh B, Sharma D K, Kumar R and Gupta A 2009 Controlled release of the fungicide thiram from starch–alginate–clay based formulation *Appl Clay Sci* **45** 76–82
[30] Lozano-Vazquez G, Lobato-Calleros C, Escalona-Buendia H, Chavez G, Alvarez-Ramirez J and Vernon-Carter E J J 2015 Effect of the weight ratio of alginate-modified tapioca starch on the physicochemical properties and release kinetics of chlorogenic acid containing beads *Food Hydrocoll* **48** 301–11
[31] Mishra S, Bajpai J and Bajpai A K 2004 Evaluation of the water sorption and controlled-release potential of binary polymeric beads of starch and alginate loaded with potassium nitrate as an agrochemical *J Appl Polym Sci* **94** 1815–26
[32] Singh B, Sharma D K and Gupta A 2009 A study towards release dynamics of thiram fungicide from starch-alginate beads to control environmental and health hazards *J Hazard Mater* **161** 208–16
[33] da Silva Fernandes R, Tanaka F N, de Moura M R and Aouada F A 2019 Development of alginate/starch-based hydrogels crosslinked with different ions: Hydrophilic, kinetic and spectroscopic properties *Mater Today Commun* **21** 100636
[34] Feng J, Dou J, Zhang Y, Wu Z, Yin D and Wu W 2020 Thermosensitive hydrogel for encapsulation and controlled release of biocontrol agents to prevent peanut aflatoxin contamination *Polymers (Basel)* **12** 547
[35] Weerapoprasit C and Prachayawarakorn J 2016 Properties of biodegradable thermoplastic cassava starch/sodium alginate composites prepared from injection molding *Polym Compos* **37** 3365–72

[36] Onyido I, Sha'Ato R and Nnamonu L A 2012 Environmentally friendly formulations of trifluralin based on alginate modified starch *J Environ Prot (Irvine, Calif)* **03** 1085–93
[37] Siddaramaiah, Raj B and Somashekar R 2004 Structure-property relation in polyvinyl alcohol/starch composites *J Appl Polym Sci* **91** 630–5
[38] Siddaramaiah, Swamy T M M, Ramaraj B and Lee J H 2008 Sodium alginate and its blends with starch: thermal and morphological properties *J Appl Polym Sci* **109** 4075–81
[39] Nandiyanto A B D, Oktiani R and Ragadhita R 2019 How to read and interpret ftir spectroscope of organic material *Indonesian Journal of Science and Technology* **4** 97–118
[40] Song B, Liang H, Sun R, Peng P, Jiang Y and She D 2020 Hydrogel synthesis based on lignin/sodium alginate and application in agriculture *Int J Biol Macromol* **144** 219–30
[41] Sheela T, Bhajantri R F, Ravindrachary V, Pujari P K, Rathod S G and Naik J 2014 Ionic conductivity studies in crystalline PVA/NaAlg polymer blend electrolyte doped with alkali salt KCl *AIP Conference Proceedings* vol 1591 (American Institute of PhysicsAIP) pp 202–4
[42] Jain A A, Mehra A and Ranade V V. 2016 Processing of TGA data: analysis of isoconversional and model fitting methods *Fuel* **165** 490–8
[43] Marie Arockianathan P, Sekar S, Sankar S, Kumaran B and Sastry T P 2012 Evaluation of biocomposite films containing alginate and sago starch impregnated with silver nano particles *Carbohydr Polym* **90** 717–24
[44] Mousavi S N, Daneshvar H, Seyed Dorraji M S, Ghasempour Z, Panahi-Azar V and Ehsani A 2021 Starch/alginate/ Cu-g-C_3N_4 nanocomposite film for food packaging *Mater Chem Phys* **267** 124583
[45] Jumaidin R, Sapuan S M, Jawaid M, Ishak M R and Sahari J 2017 Effect of seaweed on mechanical, thermal, and biodegradation properties of thermoplastic sugar palm starch/agar composites *Int J Biol Macromol* **99** 265–73
[46] Feng J, Dou J, Wu Z, Yin D and Wu W 2019 Controlled release of biological control agents for preventing aflatoxin contamination from starch–alginate beads *Molecules 2019, Vol. 24, Page 1858* **24** 1858